

Los Alamos National Laboratory is operated by the University of California for the United States Department of Energy under contract W-7405-ENG-36

**TITLE  $ZrO_2$  Reinforced- $MoSi_2$  Matrix Composites**

**AUTHOR(S)** J. J. Petrovic  
R. E. Honnell  
T. E. Mitchell  
R. K. Wade  
K. J. McClellan

**SUBMITTED TO** Proceedings, 15th Annual Conference on Composites and  
Advanced Ceramics 13-16 January 1991  
Cocoa Beach, Florida

**DISCLAIMER**

This report was prepared as an account of work sponsored by an agency of the United States Government. Neither the United States Government nor any agency thereof, nor any of their employees, makes any warranty, express or implied, or assumes any legal liability or responsibility for the accuracy, completeness, or usefulness of any information, apparatus, product, or process disclosed, or represents that its use would not infringe privately owned rights. Reference herein to any specific commercial product, process, or service by trade name, trademark, manufacturer, or otherwise does not necessarily constitute or imply its endorsement, recommendation, or favoring by the United States Government or any agency thereof. The views and opinions of authors expressed herein do not necessarily state or reflect those of the United States Government or any agency thereof.

By distribution of this article, the publisher recognizes that the U.S. Government retains a certain non-exclusive, royalty-free license to publish or reproduce the copyrighted form of this contribution or to allow others to do so for U.S. Government purposes.

The Los Alamos National Laboratory requests that the publisher identify this article as work performed under the auspices of the U.S. Department of Energy.

**Los Alamos** Los Alamos National Laboratory  
Los Alamos, New Mexico 87545

**DISTRIBUTION OF THIS DOCUMENT IS UNLIMITED**  
MASTER

# ZrO<sub>2</sub> REINFORCED-MoSi<sub>2</sub> MATRIX COMPOSITES

J.J. Petrovic, R.E. Honnell, T.E. Mitchell  
Ceramic Science & Technology Group, Los Alamos National Laboratory,  
Los Alamos, New Mexico 87545

R.K. Wade  
Arizona Materials Laboratory, University of Arizona, Tucson, Arizona  
85721

K.J. McClellan  
Department of Materials Science & Engineering, Case Western Reserve  
University, Cleveland, Ohio 44106

## ABSTRACT:

ZrO<sub>2</sub> particle-MoSi<sub>2</sub> matrix composites were fabricated by wet processing/hot pressing, using high quality unstabilized, partially stabilized, and fully stabilized ZrO<sub>2</sub> powders. Composite room temperature indentation fracture toughness increased with increasing volume fraction of ZrO<sub>2</sub> reinforcement. Unstabilized ZrO<sub>2</sub> produced the highest composite fracture toughness, 7.8 MPa m<sup>1/2</sup> as compared to 2.6 MPa m<sup>1/2</sup> for pure MoSi<sub>2</sub>. Unstabilized ZrO<sub>2</sub> composites exhibited matrix microcracking, and the spontaneous tetragonal-to-monoclinic ZrO<sub>2</sub> phase transformation induced significant plastic deformation in the MoSi<sub>2</sub> matrix. Partially stabilized ZrO<sub>2</sub> produced a lesser extent of composite fracture toughening, possibly as a result of an inhomogeneous ZrO<sub>2</sub> particle distribution and presence of a glassy phase.

## INTRODUCTION:

The intermetallic compound  $\text{MoSi}_2$  possesses an interesting set of properties which make it a candidate matrix material for high temperature structural composites. It has a high melting point of 2030 C, and possesses excellent high temperature oxidation resistance due to the formation of a protective silica phase. Unlike structural ceramics, this material exhibits a brittle-to-ductile transition at 900-1000 C. Below this temperature it is brittle, but above this temperature it deforms extensively by dislocation plasticity.  $\text{MoSi}_2$  is thermodynamically stable with a number of important ceramic materials, including  $\text{SiC}$ ,  $\text{ZrO}_2$ ,  $\text{Si}_3\text{N}_4$ ,  $\text{Al}_2\text{O}_3$ ,  $\text{TiB}_2$ ,  $\text{TiC}$ , and  $\text{ZrB}_2$ . It also has the potential for alloying with other high melting point silicides, such as  $\text{WSi}_2$ ,  $\text{Mo}_5\text{Si}_3$ , and  $\text{Ti}_5\text{Si}_3$ . This material poses no health hazards, and is environmentally benign. Finally, the electrical conductivity of  $\text{MoSi}_2$  is such that it can be electro-discharge machined (EDM), a potentially advantageous cost factor for the fabrication of components from the material.

Of itself,  $\text{MoSi}_2$  is not considered to be a structural material, due to its room temperature brittleness and its low strength levels at elevated temperatures. It has, however, attained significant application as a heating element material for furnaces operating in air to 1800 C, which attests to its excellent environmental stability under oxidizing conditions.

For  $\text{MoSi}_2$  to be employed as an oxidation-resistant elevated temperature structural material, both its high temperature strength and creep resistance and its room temperature fracture toughness must be significantly improved. This can be accomplished through the composite approach. However, it is important that composite strategies pursued do not degrade the oxidation resistance significantly.

Previous work has demonstrated that  $\text{SiC}$  composite reinforcements and  $\text{WSi}_2$  matrix alloying can markedly improve the elevated temperature mechanical properties of  $\text{SiC-MoSi}_2$  based composites (1-7). Additionally, the feasibility of utilizing  $\text{ZrO}_2$  transformation toughening to significantly improve the room temperature fracture toughness of  $\text{ZrO}_2$  particle- $\text{MoSi}_2$  matrix composites has recently been demonstrated (8).

The purpose of the present investigation was to explore microstructure-mechanical property aspects in more detail, in a second

generation of  $\text{ZrO}_2$ - $\text{MoSi}_2$  composites fabricated using high quality  $\text{ZrO}_2$  powders. Of primary interest were initial assessments of effects of  $\text{ZrO}_2$  phase stability and volume fraction on composite microstructures, substructures, and fracture toughness.

### $\text{ZrO}_2$ REINFORCEMENT OF $\text{MoSi}_2$ :

$\text{ZrO}_2$  is a potentially important reinforcing species for  $\text{MoSi}_2$ . This material presents the possibility of utilizing transformation toughening effects to significantly improve the room temperature fracture toughness of  $\text{MoSi}_2$  based composites (8). In addition, there is also the possibility of deriving elevated temperature  $\text{ZrO}_2$  dispersion strengthening effects. The chemical species  $\text{ZrO}_2$  and  $\text{MoSi}_2$  are stable with each other under inert conditions. The thermal expansion coefficient of  $\text{ZrO}_2$  is a reasonably good match with that of  $\text{MoSi}_2$ , allowing flexibility in composite system design. Finally, the presence of  $\text{ZrO}_2$  does not greatly degrade composite oxidation resistance (9).

### EXPERIMENTAL:

#### Fabrication of $\text{ZrO}_2$ Particle- $\text{MoSi}_2$ Matrix Composites:

A range of commercial  $\text{ZrO}_2$  powders from the Tosoh Corporation were employed in the investigation. Powders containing 0, 2, 2.5, 3, 4, and 8 mole %  $\text{Y}_2\text{O}_3$  were evaluated. The 0 mole %  $\text{Y}_2\text{O}_3$  material is unstabilized pure  $\text{ZrO}_2$ . The range of 2-4 mole %  $\text{Y}_2\text{O}_3$  constitutes partially stabilized  $\text{ZrO}_2$ . The 8 mole %  $\text{Y}_2\text{O}_3$  is fully stabilized  $\text{ZrO}_2$ .  $\text{ZrO}_2$  powders partially stabilized with 9 mole %  $\text{MgO}$  and 12 mole %  $\text{CeO}_2$  were also examined. All Tosoh powders were high purity, with an average particle size of 0.3 micron.

The  $\text{MoSi}_2$  powder employed was commercial powder from the Alfa Corporation. This powder was screened to -400 mesh prior to mixing with the various  $\text{ZrO}_2$  powders.  $\text{ZrO}_2$  and  $\text{MoSi}_2$  powders were co-dispersed in an aqueous media at a pH of 2.5. Mechanical stirring and ultrasonification were employed. The solids loading was 60 wt. %.

The powder co-dispersion was slip cast into a plaster of paris mold, and the slip cast body crushed into -100 mesh feed powder for hot pressing. Hot pressing consolidation of composites was performed at 1700 C and 32 MPa pressure, using grafoil-lined graphite dies and an argon atmosphere. Hot pressed composites were 94-95% dense.

#### Indentation Fracture Toughness:

Microhardness indentation techniques were employed to determine the room temperature fracture toughness of the various  $\text{ZrO}_2\text{-MoSi}_2$  composites. A 10 kg Vickers indentation was employed, and the approach of Anstis et. al. (10) was used to calculate fracture toughness values.

#### Transmission Electron Microscopy:

Thin foils for TEM were prepared as follows. A 250 micron thick slice was cut from the hot pressed disc, taking care to avoid the edges of the disc in order to minimize any surface effects such as contamination or density gradients. The slice was then ground and polished on one side to a thickness of about 150 microns, with the final polish using 1 micron diamond paste. Discs were cut from the center of the slice and mounted on Cu grids for support. The unfinished side was ground and polished to a thickness of about 50 microns. The thin section was dimpled with a 10 gm load and 1 micron diamond paste to a final thickness of less than 25 microns. The foil was then ion thinned to perforation using Ar ions. TEM studies of the microstructure and dislocation structures were performed using a Philips CM30 SEM at 400 keV

### RESULTS AND DISCUSSION:

#### Indentation Fracture Toughness:

Fracture toughness as a function of mole %  $\text{Y}_2\text{O}_3$  stabilizer for 20 vol.%  $\text{ZrO}_2$  reinforcement of the  $\text{MoSi}_2$  matrix is shown in Figure 1. Also shown are results for the  $\text{MgO}$  and  $\text{CeO}_2$  stabilized  $\text{ZrO}_2$  reinforcements. As may be seen, the maximum toughness was observed for unstabilized  $\text{ZrO}_2$  (0 mole %  $\text{Y}_2\text{O}_3$ ). For this case, a room

temperature toughness value of  $7.8 \text{ MPa m}^{1/2}$  was observed, as compared to a value of  $2.6 \text{ MPa m}^{1/2}$  for pure  $\text{MoSi}_2$ . Partially stabilized (2-4 mole %  $\text{Y}_2\text{O}_3$ ) compositions and fully stabilized  $\text{ZrO}_2$  (8 mole %  $\text{Y}_2\text{O}_3$ ) exhibited lower toughness values.  $\text{MgO}$  and  $\text{CeO}_2$  stabilized materials yielded toughness levels slightly higher than the  $\text{Y}_2\text{O}_3$  stabilized materials.

Composite fracture toughness as a function of volume %  $\text{ZrO}_2$  reinforcement is shown in Figure 2. In this case the  $\text{ZrO}_2$  composition was a partially stabilized one containing 2.5 mole %  $\text{Y}_2\text{O}_3$ . One may see that the fracture toughness increases roughly linearly with increasing partially stabilized  $\text{ZrO}_2$  content, from pure  $\text{MoSi}_2$  to pure partially stabilized  $\text{ZrO}_2$ .

#### Microstructures:

Composite microstructures and the nature of indentation cracks are shown in Figure 3, for  $\text{ZrO}_2$  reinforcements stabilized with  $\text{Y}_2\text{O}_3$ . A significant amount of grain boundary microcracking was observed in the 0%  $\text{Y}_2\text{O}_3$  (unstabilized  $\text{ZrO}_2$ ) composite, with little or no microcracking observed in the partially stabilized (2-4%  $\text{Y}_2\text{O}_3$ ) or fully stabilized (8%  $\text{Y}_2\text{O}_3$ ) materials. It may also be noted that cracks tended to run through both the  $\text{ZrO}_2$  and  $\text{MoSi}_2$  phases, without exhibiting a preference for the phase boundaries. Significant microcracking was also observed in the  $\text{MgO}$  and  $\text{CeO}_2$  stabilized composites.

#### Transmission Electron Microscopy:

Transmission electron microscopy results are summarized in Table 1. The microstructures of the various materials all showed a heterogeneous distribution of  $\text{ZrO}_2$  within the  $\text{MoSi}_2$  matrix, which typically involved intergranular pockets of  $\text{ZrO}_2$  grains. There was also a relatively large amount of a silicate glassy phase present within the pockets, which wetted the  $\text{ZrO}_2$ - $\text{ZrO}_2$  grain boundaries. The intergranular  $\text{ZrO}_2$  grain size varied between 1 and 6 microns. There were a small number of intragranular  $\text{ZrO}_2$  grains which were submicron in size. There

was no evidence of any chemical reaction between  $\text{ZrO}_2$  and  $\text{MoSi}_2$  in the as-fabricated composite specimens examined.

Representative transmission electron micrographs of the unstabilized (0%  $\text{Y}_2\text{O}_3$ ), partially stabilized (2.5%  $\text{Y}_2\text{O}_3$ ), and fully stabilized (8%  $\text{Y}_2\text{O}_3$ )  $\text{ZrO}_2$  reinforced- $\text{MoSi}_2$  matrix composites are shown in Figures 4-6, respectively. These may be correlated with the observations in Table 1.

For the unstabilized  $\text{ZrO}_2$  material, one may note in Figure 4 the presence of grain boundary microcracking in the  $\text{MoSi}_2$ , as well as a high dislocation density in the  $\text{MoSi}_2$ . The high  $\text{MoSi}_2$  dislocation density is particularly intriguing. This results because the tetragonal-to-monoclinic phase transformation temperature is above the brittle-to-ductile transition temperature of  $\text{MoSi}_2$ . Thus, the volume change associated with the  $\text{ZrO}_2$  transformation effectively "pumps" dislocations into the  $\text{MoSi}_2$  phase. These dislocations were observed to have predominantly  $\langle 100 \rangle$  type Burgers vectors. Microcracking also occurs, since the  $\text{MoSi}_2$  plasticity apparently cannot accommodate all of the transformation strain. Both of these factors, a high  $\text{MoSi}_2$  dislocation density and  $\text{MoSi}_2$  microcracking, are likely the primary contributors to the high value of fracture toughness observed for the unstabilized  $\text{ZrO}_2$  composite in Figure 1.

For the partially stabilized and fully stabilized  $\text{ZrO}_2$ ,  $\text{MoSi}_2$  dislocation densities were observed to be much lower than for the unstabilized  $\text{ZrO}_2$  case. This is due to the fact that no  $\text{ZrO}_2$  phase transformations occurred in these materials upon cooling from the composite fabrication temperature. The glassy phase and inhomogeneity of the  $\text{ZrO}_2$  particle distribution are evident in Figures 5 and 6. It is likely that these characteristics of the partially stabilized  $\text{ZrO}_2$  composites, namely a non-uniform  $\text{ZrO}_2$  particle distribution and the presence of a glassy phase, may have contributed to the relatively low values of fracture toughness observed in Figure 1. This suggests that possible routes to more fully exploiting crack-tip-induced transformation toughening in  $\text{ZrO}_2$ - $\text{MoSi}_2$  composites may be to improve the dispersion of  $\text{ZrO}_2$  particle in the  $\text{MoSi}_2$  matrix, and minimize/eliminate the glassy phase.

## CONCLUSIONS:

ZrO<sub>2</sub> particle-MoSi<sub>2</sub> matrix composites were fabricated by wet processing and hot pressing, using high quality ZrO<sub>2</sub> powders. Unstabilized, partially stabilized, and fully stabilized ZrO<sub>2</sub> was examined. Hot pressing was performed at 1700 C, and hot pressed composites were 94-95% dense.

The room temperature indentation fracture toughness of ZrO<sub>2</sub>-MoSi<sub>2</sub> composites increased with increasing volume fraction of ZrO<sub>2</sub>. Unstabilized ZrO<sub>2</sub> was observed to produce the highest composite fracture toughness, 7.8 MPa m<sup>1/2</sup> as compared to 2.6 MPa m<sup>1/2</sup> for pure MoSi<sub>2</sub>. Matrix microcracking was prominently observed for unstabilized ZrO<sub>2</sub>. In addition, the spontaneous tetragonal-to-monoclinic ZrO<sub>2</sub> phase transformation in unstabilized ZrO<sub>2</sub> produced significant plastic deformation in the MoSi<sub>2</sub> matrix.

Partially stabilized ZrO<sub>2</sub> produced a lower degree of fracture toughening of the composite in comparison to unstabilized ZrO<sub>2</sub>. This suggests that crack tip-induced transformation toughening was not fully operational in the present composites. Observations of an inhomogeneous distribution of ZrO<sub>2</sub> particles and the presence of a glassy phase may have been contributing factors inhibiting the full operation of toughening mechanisms for partially stabilized ZrO<sub>2</sub>.

## ACKNOWLEDGEMENTS:

The authors gratefully acknowledge the DOE/Advanced Industrial Materials Program for support of the present investigation.

## REFERENCES:

1. J.J. Petrovic and R.E. Honnell, "SiC Reinforced-MoSi<sub>2</sub>/WSi<sub>2</sub> Alloy Matrix Composites", Ceram. Eng. Sci. Proc., 11 (1990), 734-744.

2. O. Unal, J.J. Petrovic, D.H. Carter, and T.E. Mitchell, "Dislocations and Plastic Deformation in Molybdenum Disilicide", J. Am. Ceram. Soc., 73 (1990), 1752-1757.
3. J.J. Petrovic, R.E. Honnell, and A.K. Vasudevan, "SiC Reinforced-MoSi<sub>2</sub> Alloy Matrix Composites", Mat. Res. Soc. Symp. Proc. Vol. 19 (1990), 123-130.
4. J.J. Petrovic and R.E. Honnell, "SiC Reinforced-MoSi<sub>2</sub> Based Matrix Composites", Proceedings, Symposium on Ceramic, Polymer and Metal Matrix Composites, American Ceramic Society Second International Ceramic Science and Technology Congress, 12-15 November 1990, Orlando, Florida.
5. J.J. Petrovic and R.E. Honnell, "MoSi<sub>2</sub> Particle Reinforced-SiC and Si<sub>3</sub>N<sub>4</sub> Matrix Composites", J. Mat. Sci. Lett., 9 (1990), 1083-1084.
6. A.K. Bhattacharya and J.J. Petrovic, "Hardness and Fracture Toughness of SiC Particle-Reinforced MoSi<sub>2</sub> Composites", submitted to the Journal of the American Ceramic Society, 1991.
7. K. Sadananda, H. Jones, J. Feng, J.J. Petrovic, and A.K. Vasudevan, "Creep of Monolithic and SiC Whisker Reinforced MoSi<sub>2</sub>", Proceedings, 15th Annual Conference on Composites and Advanced Ceramics, American Ceramic Society, January 1991, Cocoa Beach, Florida.
8. J.J. Petrovic and R.E. Honnell, "Partially Stabilized ZrO<sub>2</sub> Particle-MoSi<sub>2</sub> Matrix Composites", J. Mat. Sci., 25 (1990), 4453-4456.
9. Wayne L. Worrell, University of Pennsylvania, private communication.
10. G.R. Anstis, P. Chantikul, B.R. Lawn, and D.B. Marshall, J. Am. Ceram. Soc., 64 (1981), 533-538.

**Table 1: Summary of transmission electron microscopy observations for ZrO<sub>2</sub> particle-MoSi<sub>2</sub> matrix composites containing 20 vol. % ZrO<sub>2</sub> reinforcement.**

<b>Stabilizer (mole %)</b>	<b>ZrO<sub>2</sub> Polymorph (room temp)</b>	<b>Dislocation Density (apparent)</b>	<b>Microcracking (intergranular)</b>
0.0 Y <sub>2</sub> O <sub>3</sub>	Monoclinic	High	High
2.5 Y <sub>2</sub> O <sub>3</sub>	Tetragonal	Low	Low
4.0 Y <sub>2</sub> O <sub>3</sub>	Tetragonal	Low	Low
8.0 Y <sub>2</sub> O <sub>3</sub>	Cubic	Very Low	Very Low
12 CeO <sub>2</sub>	Monoclinic	High	Very High
9.0 MgO	Monoclinic	High	High

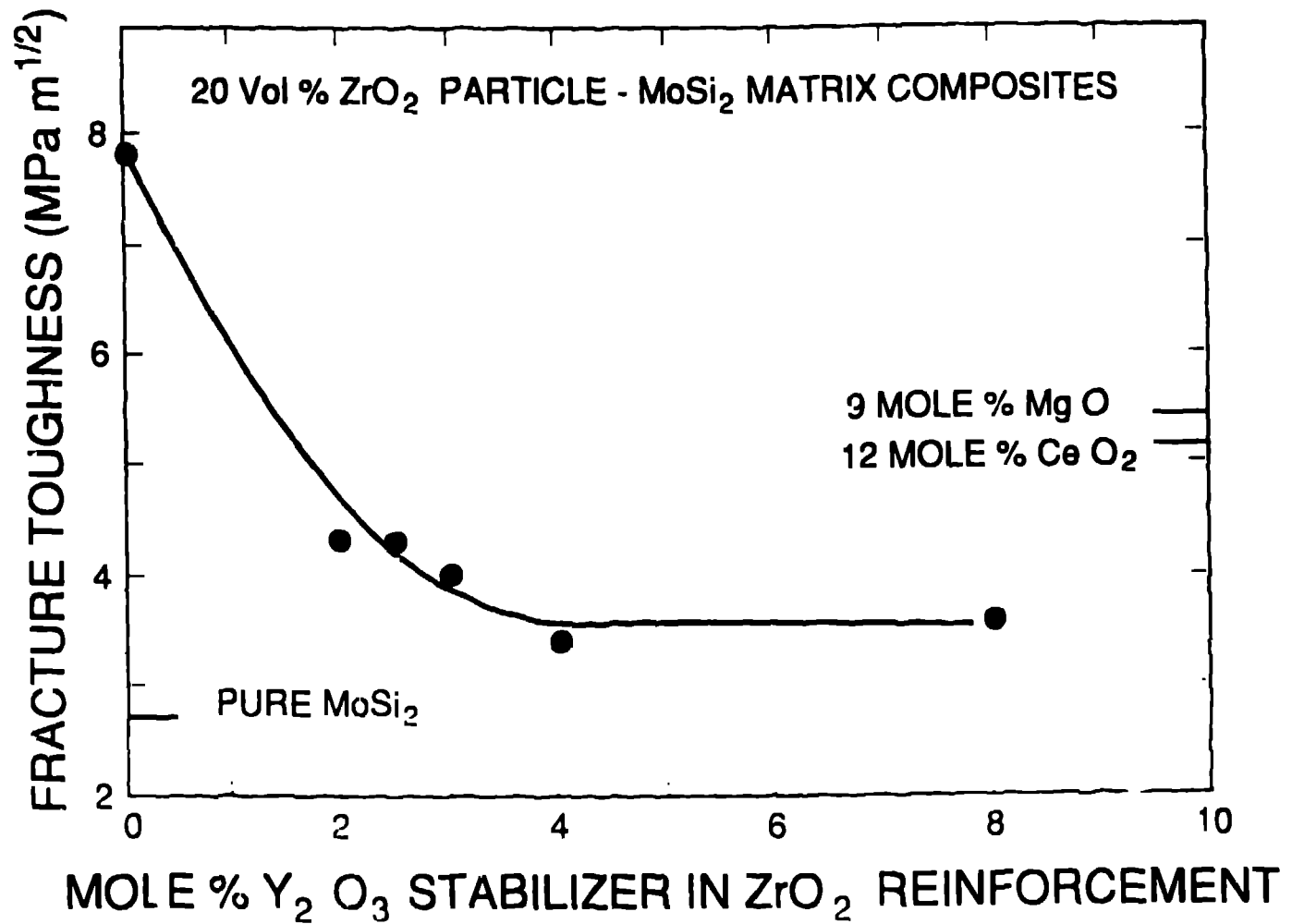


Figure 1: Room temperature fracture toughness of 20 vol.%  $\text{ZrO}_2$  particle- $\text{MoSi}_2$  matrix composites, as a function of mole %  $\text{Y}_2\text{O}_3$  stabilizer in the  $\text{ZrO}_2$  reinforcement.

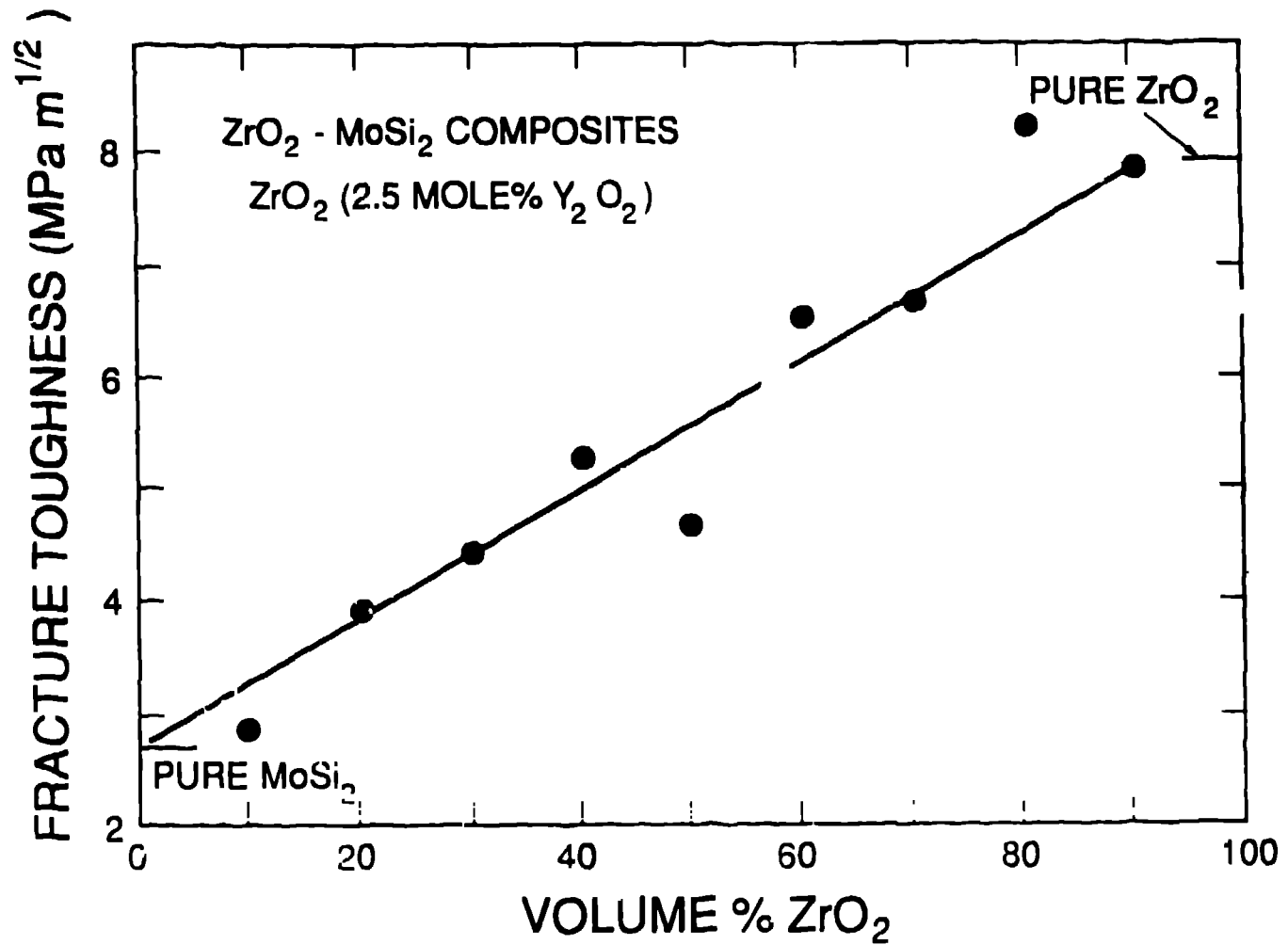


Figure 2: Fracture toughness of ZrO<sub>2</sub> reinforced-MoSi<sub>2</sub> matrix composites as a function of ZrO<sub>2</sub> volume %. The ZrO<sub>2</sub> is partially stabilized with 2.5 mole % Y<sub>2</sub>O<sub>3</sub>.

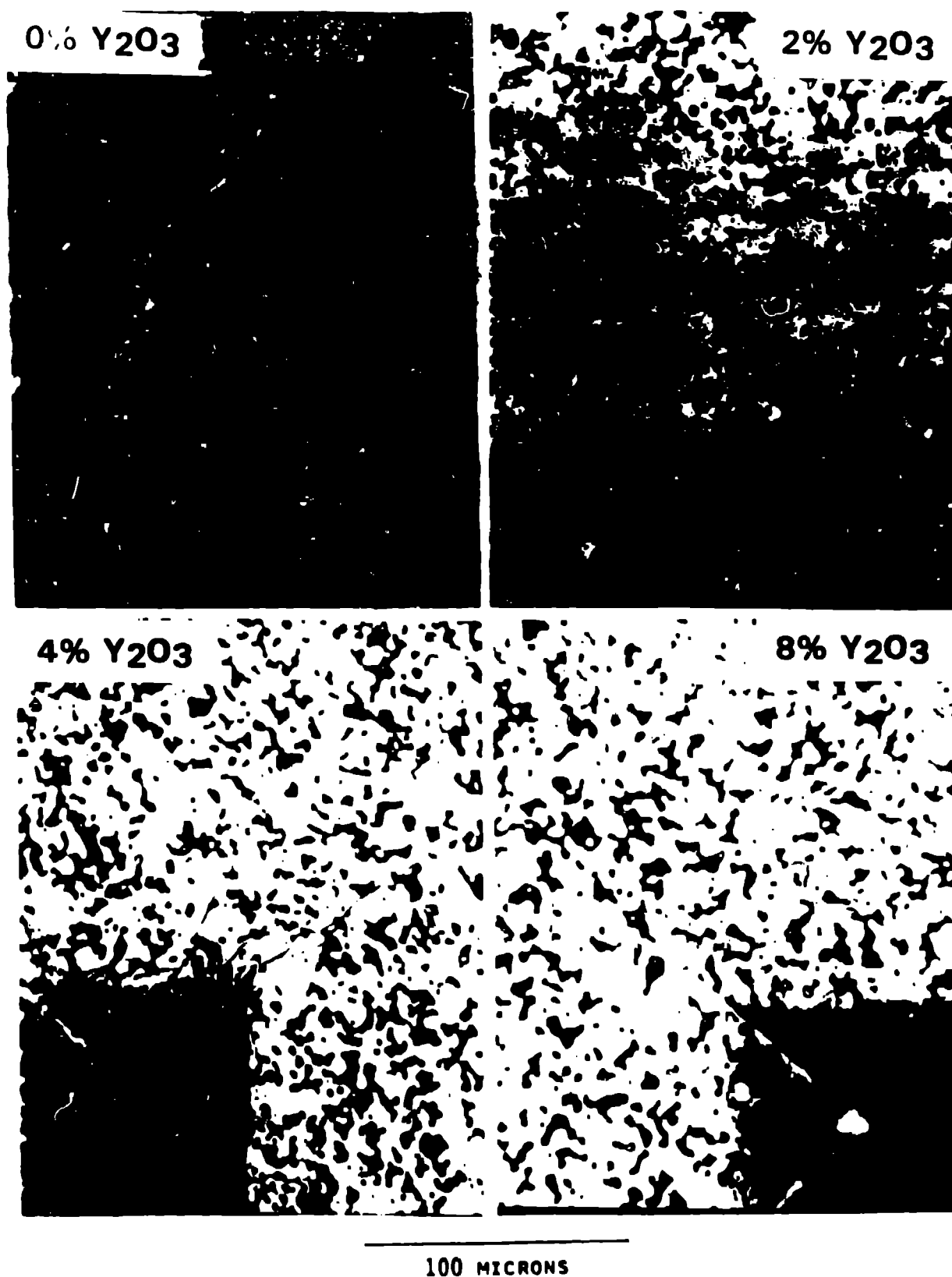


Figure 3: Microstructures of 20 vol.%  $ZrO_2(Y_2O_3)$  reinforced- $MoSi_2$  matrix composites, showing indentation crack morphologies.

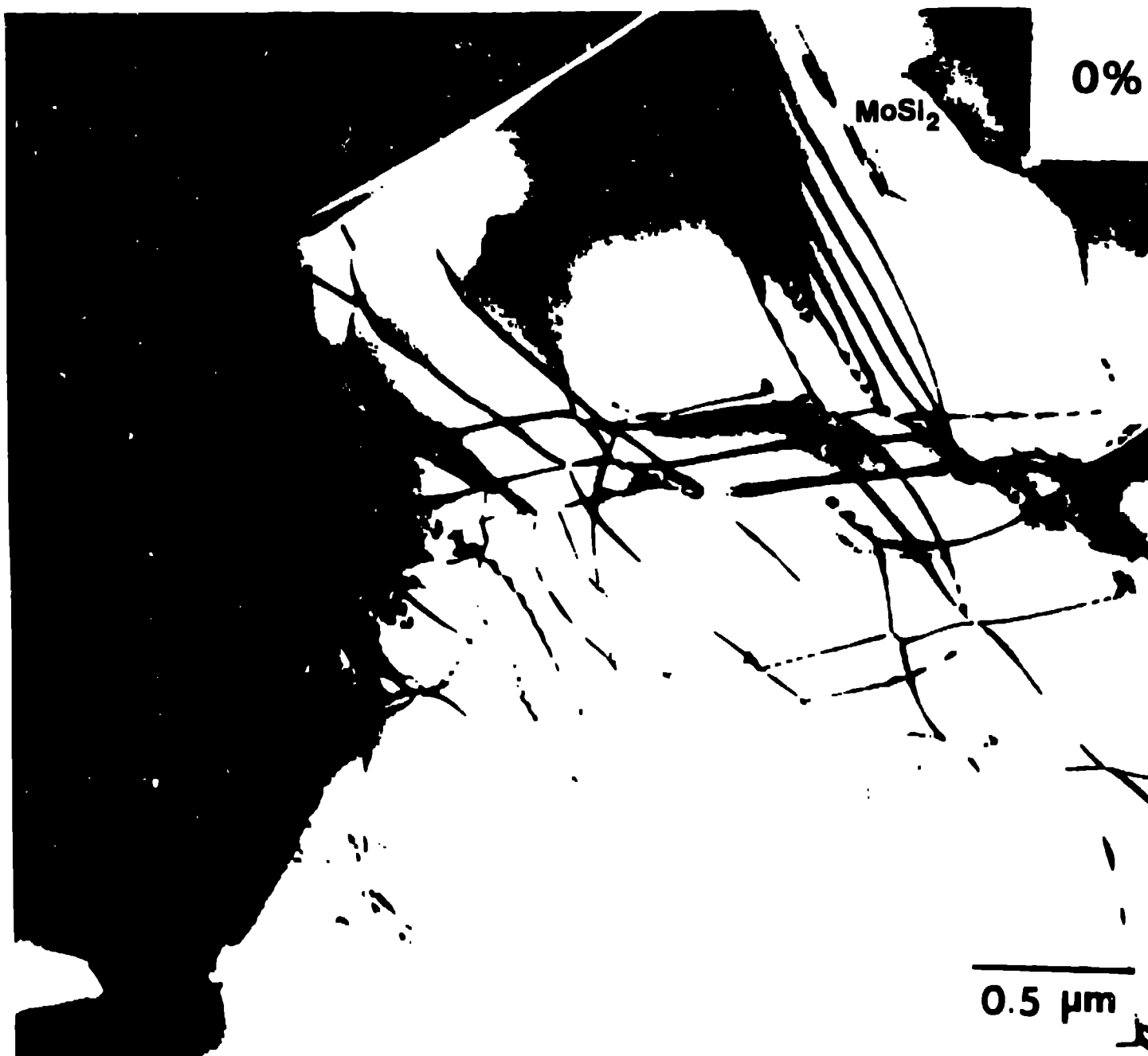


Figure 4: Transmission electron micrograph of 20 vol.% unstabilized  $ZrO_2$  (0%  $Y_2O_3$ )  $MoSi_2$  matrix composite.



Figure 5: Transmission electron micrograph of 20 vol.% partially stabilized ZrO<sub>2</sub> (2.5% Y<sub>2</sub>O<sub>3</sub>)-MoSi<sub>2</sub> matrix composite.

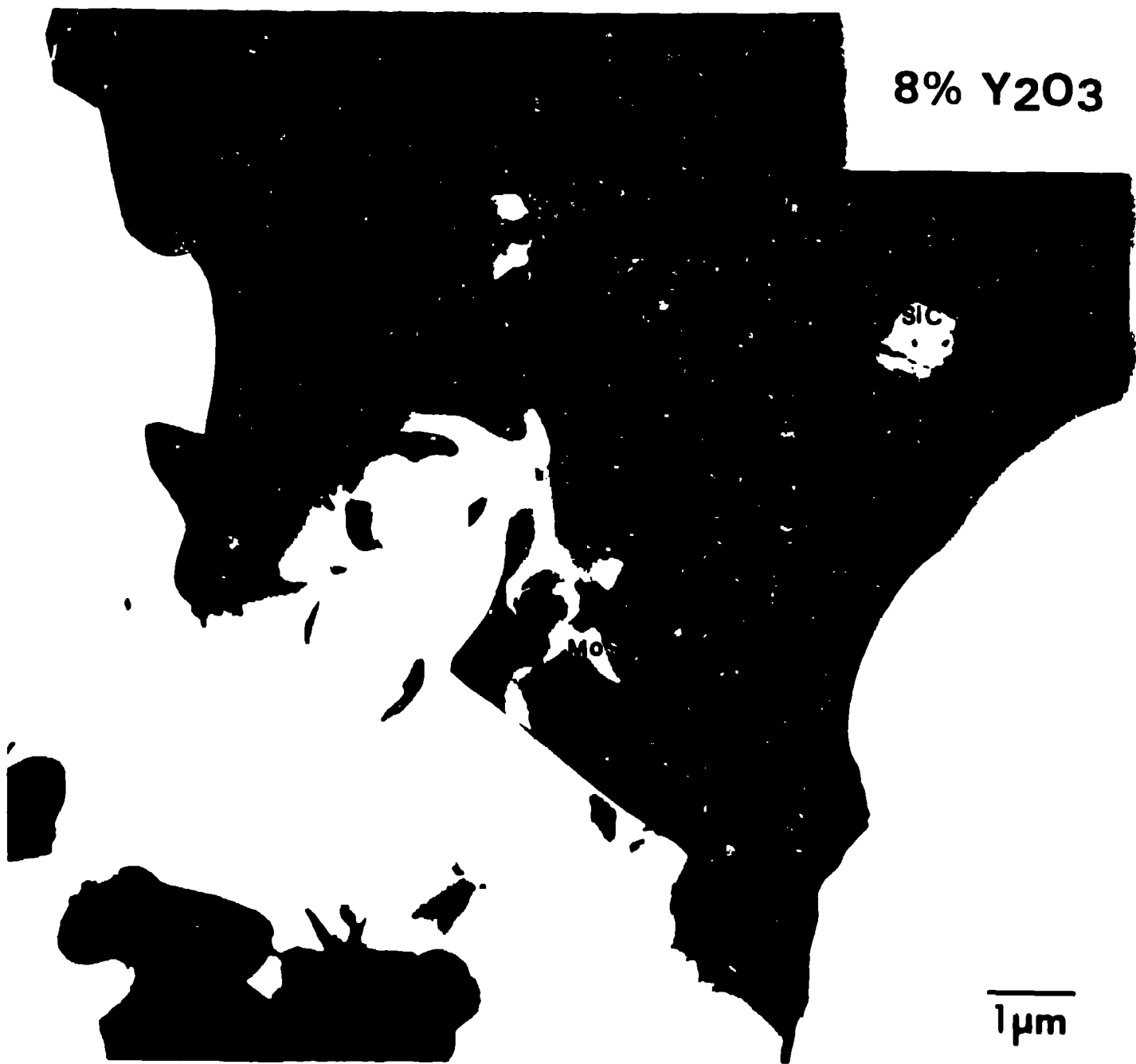


Figure 6: Transmission electron micrograph of 20 vol.% fully stabilized  $ZrO_2$  (8%  $Y_2O_3$ )  $MoSi_2$  matrix composite. Note stray SiC particle.